Video Article

Visualization of Low-Level Gamma Radiation Sources Using a Low-Cost, High-Sensitivity, Omnidirectional Compton Camera

Hiroshi Muraishi[1], Ryoji Enomoto[2], Hideaki Katagiri[3], Mika Kagaya[4], Takara Watanabe[5], Naofumi Narita[3], Daisuke Kano[5]

[1]School of Allied Health Sciences, Kitasato University

[2]Institute for Cosmic Ray Research, University of Tokyo

[3]College of Science, Ibaraki University

[4]National Institute of Technology, Sendai College

[5]National Cancer Center Hospital East

Correspondence to: Hiroshi Muraishi at muraishi@ahs.kitasato-u.ac.jp

URL: https://www.jove.com/video/60463
DOI: doi:10.3791/60463

Keywords: Environmental Sciences, Issue 155, gamma-ray imaging, Compton camera, radioactive contamination, environmental monitoring, radiation protection, Fukushima Daiichi nuclear powerplant accident

Date Published: 1/30/2020

Citation: Muraishi, H., Enomoto, R., Katagiri, H., Kagaya, M., Watanabe, T., Narita, N., Kano, D. Visualization of Low-Level Gamma Radiation Sources Using a Low-Cost, High-Sensitivity, Omnidirectional Compton Camera. *J. Vis. Exp.* (155), e60463, doi:10.3791/60463 (2020).

Abstract

We present experimental protocols for visualizing various low-level gamma radiation sources in the ambient environment. Experiments were conducted by using a low-cost, high-sensitivity, omnidirectional, gamma-ray imaging Compton camera. In the laboratory, the position of a sub-MeV gamma radiation source such as ^{137}Cs can easily be monitored via omnidirectional gamma-ray imaging obtained by the Compton camera. In contrast, a stationary, wall-mounted dose rate monitor cannot always successfully monitor such a source. Furthermore, we successfully demonstrated the possibility of visualizing the radioactivity movement in the environment, for example, the movement of a patient injected with ^{18}F-fluorodeoxyglucose (^{18}F-FDG) in a nuclear medicine facility. In the Fukushima field, we easily obtained omnidirectional gamma-ray images concerned with the distribution on the ground of low-level radioactive contamination by radioactive cesium released by the Fukushima Daiichi nuclear power plant accident in 2011. We demonstrate clear advantages of using our procedure with this camera to visualize gamma-ray sources. Our protocols can further be used to discover low-level gamma radiation sources, in place of stationary dose rate monitors and/or portable survey meters used conventionally.

Video Link

The video component of this article can be found at https://www.jove.com/video/60463/

Introduction

Medical facilities house various low-level gamma radiation sources with a surface and/or air dose rate of just a few μSv/h. Such sources are also present across broad areas of eastern Japan exhibiting low-level radioactive contamination by radioactive cesium from the Fukushima Daiichi nuclear power plant accident in 2011. These environments sometimes expose workers to the external irradiation exposure limit for the human body for the general population as advised by the International commission on radiological protection (ICRP): 1 mSv/year (e.g., 1 μSv/h for 4 h per day, 250 days per year)[1]. If radiation sources are visualized from more than a few meters in advance on short timescales, the amount of radiation exposure can be reduced. One of the best solutions for visualizing these gamma radiation sources is to adopt a gamma-ray imaging Compton camera technique[2]. In this technique, the energy and cone-direction of incident gamma-rays emitted from the radiation source are measured by the detector for each event, and then the gamma-ray source direction can be reconstructed by back-projection[3]. Previous studies have developed Compton camera systems aimed at the application of a new diagnostic device in nuclear medicine and/or a new gamma-ray telescope in astrophysics[4,5,6,7,8,9,10,11,12,13,14], as well as image reconstruction techniques for Compton cone data by analytical[15,16] and statistical[17] approaches. More expensive, state-of-the-art devices with complicated electronics are often adopted to obtain high angular resolution within a standard deviation of a few degrees, but this precision makes it difficult to simultaneously achieve high detection efficiency.

Recently, we have proposed and developed a low-cost, high-sensitivity, omnidirectional gamma-ray imaging Compton camera[18], based on a two-fold coincidence within a number of independent scintillators that act as either scatterers or absorbers[19]. The aim of this technique is to easily achieve high detection efficiency with an angular resolution s of ~10 degrees or less, which is adequate for an environmental monitor. This is accomplished through the application of an image-sharpening technique[18,20] based on the filtered back-projection algorithm, which applies a convolution filter used in image reconstruction for computed tomography to the Compton reconstruction. Furthermore, the detection efficiency, angular resolution and dynamic range of the detector can be easily optimized when the type, size and arrangement of scintillators are coordinated in accordance with a particular purpose, such as usage in environments emitting elevated radioactivity[21,22].

In this study, we present experimental protocols for various trials for visualizing low-level gamma-ray radiation sources using this omnidirectional Compton camera technique in a radioisotope (RI) facility, a positron emission tomography (PET) facility and the Fukushima field. We prepared and utilized the omnidirectional gamma-ray imaging Compton camera previously developed by ourselves[18] but with some improvements, in order to achieve higher detection efficiency. **Figure 1** shows a schematic view of the arrangement of CsI(Tl) scintillators of eleven elements used in this study. The eleven counters consist of two layers; two counters at the center and nine counters in a half-circle, considering forward and backward scattering configurations. Each CsI(Tl) scintillator cube of 3.5 cm was read out with super-bialkali photo-multiplier tubes (PMT). The signals were fed into a flash ADC board with SiTCP technology[23] and the front end was connected to a PC via Ethernet. An online program created using Visual C++ with ROOT library[24] was operated on a Windows PC. A gamma-ray image was reconstructed and sharpened[18,20] on a spherical surface with accumulating rings with a radius of θ that is a scattering angle calculated from Compton kinematics for each two-fold coincidence event. An omnidirectional gamma-ray image can be displayed both online and offline by superimposition on the omnidirectional optical image previously taken by a digital camera. During the measurement, the trigger rate, total energy spectrum (the sum of the energy deposits for each two-fold coincidence event), and the reconstructed images of a preset gamma-ray energy can be displayed on the online PC screen. This information can be updated at a preset time interval (e.g., every 10 s). Here, we set the screen to display two types of reconstructed images: an image that is accumulated at the start of the measurement and an image reaccumulated at every preset time interval (e.g., every 1 min). Furthermore, because the raw data for each event obtained using the measurements are stored, it is possible to reanalyze the data after the measurements and then regenerate a reconstructed image for an arbitrary gamma-ray energy at an arbitrary time interval. **Table 1** shows the performance of the Compton camera system used in this study, by comparison with the previous six-counter system[18]. The comparison revealed that a sub-MeV gamma-ray source was successfully visualized with a detection efficiency twice that of the previous system, while maintaining the angular resolution s of ~11 degrees. We also confirmed that the angular dependence of acceptance was kept to a minimum, showing differences of s ~ 4%. The details on the fundamental techniques of the system are described in Watanabe et al. (2018)[18]. Here we introduce three experimental protocols for visualizing various low-level gamma-ray radiation sources using the Compton camera described above.

Protocol

The protocol was conducted following the guidelines of the research ethics committee at the National Cancer Center Hospital East, Japan.

1. Monitoring of sealed radiation source in experiment room at RI facility

1. Set the Compton camera beside the dose rate monitor as shown in **Figure 2a**. Set the height of the detectors from the ground to 2.5 m. Build the dose rate monitor, which consists of a parallel plate ionization chamber, into the upper part of the entrance of the experiment room at the RI facility to monitor the air dose rate of the position at intervals of 1 min.
2. Turn on the power of the Compton camera and online computer.
3. Start the simultaneous measurement with Compton camera and the dose rate monitor.
4. Set a ^{137}Cs sealed source (3.85 MBq) at a position labelled 'A' in **Figure 2a** and leave it for 30 min. Set the distance between the detector and the sealed source to 3.6 m.
5. Move the sealed source to a position labelled 'B' and leave it during 30 min. Set the distance between the detector and the sealed source to 6.7 m.
6. Move the sealed source at a position labelled 'C' and leave it during 30 min. Set the distance between the detector and the sealed source to 6.7 m.
7. Move the sealed source at a position labelled 'D' and leave it during 30 min. Set the distance between the detector and the sealed source to 1 m.
8. Move the sealed source outside the room. After 30 min, stop all measurement.

2. Environmental monitoring in PET facility

1. Set the Compton camera in front of reception desk in PET facility as shown in **Figure 2b**. Set the height of the detectors from the ground to 1 m.
2. Set the online computer in the staff room.
3. Turn on the power of the Compton camera and online computer.
4. Start Compton camera measurement early in the morning before patients arrive at facility.
5. After all patients leave for the day, stop all measurement.

3. Outdoor measurement in Kawamata-machi, Fukushima, Japan

1. Set the Compton camera near a private house as shown in **Figure 2c**, where the existence of some radiological Caesium hot spots with surface dose rates of 1 μSv/h or less are suspected. Set the height of the detectors from the ground to 1.5 m.
2. Turn on the power of the Compton camera and online computer.
3. Start Compton camera measurement.
4. After 30 min, stop all measurement.

Representative Results

Monitoring of sealed radiation source in experiment room at RI facility

Figure 3a shows the time variation of trigger rate measured by the Compton camera (black solid line), after applying a time-lag selection of two-hit counters less than 1 μs. The trigger rate changed every 30 min depending on the position of the sealed source (i.e., distance from the position to the camera). This variation was confirmed from the data measured by the stationary dose rate monitor (blue dashed line); the behavior remained constant (i.e., background level) other than between 5750 s and 7800 s. Here, we tentatively set five periods labelled (i), (ii), (iii), (iv) and (v), representing the five positions of the sealed source (**Figure 3a**). **Figure 3b** shows the total energy spectra for each such period (30 min for each), the horizontal axis representing the sum of energy deposits for each two-fold coincidence event. We note 662 keV photo-absorption peaks originating from the ^{137}Cs sealed source for (i), (ii), (iii) and (iv), while (v) shows only background levels. Peak heights for (ii) and (iii) are the same, which we attribute to the same 6.7 m distance from the camera to the sealed source. By selecting the event within 662±40 keV for 662 keV, we calculated the scattering angles and reconstructed the omnidirectional gamma-ray image. The results are shown in **Figures 3c-f**, respectively, for periods (i), (ii), (iii) and (iv). Here gamma-ray images are indicated by the red region, which indicates gamma-ray intensities in the upper half of the observed range. We find that the position of the ^{137}Cs sealed source can be successfully identified from the gamma-ray images. **Figure 4** shows the changes in the image with integration time, where the red field instead corresponds to a narrower range (the upper 30%) of the observed range. This narrower range was adopted in order to give priority to a peak intensity. In this case, ^{137}Cs source direction could be identified after 30 s.

Environmental monitoring in PET facility

Figure 5a shows the overall time variation of the trigger rate during the daytime (5.6 h) as measured by the Compton camera (black line) in front of a reception desk in a PET facility. We observe remarkable enhancement in the trigger rate with various patterns, which could be attributed to the movement of patients injected with ^{18}F-fluorodeoxyglucose (^{18}F-FDG) around the reception desk. As an example of such patterns, we focus on the period from 6200 s to 7000 s. According to the trigger rate in this period shown in **Figure 5b**, a series of enhancements are apparent, with two plateaus labelled (i) and (ii). **Figure 5c** shows the total energy spectra for **Figure 5b**'s periods (i), (ii) and (iii). We observe 511 keV photo-absorption peaks originating from the ^{18}F-FDG. **Figure 5d,e** show the 511 keV gamma-ray omnidirectional image in periods (i) and (ii), respectively, in which we selected events within 511±40 keV for image reconstruction. The directions of gamma-ray peaks in both figures correspond respectively to the directions of the sofa and the restroom behind the wall. Considering the trigger rates of both (i) and (ii), we interpret the gamma-rays in (i) as leakage penetrating the shield of the wall from the restroom; we presume that a patient entered the restroom and spent two minutes, and after that sat on the sofa a few minutes before the PET scan.

Outdoor measurement in Kawamata-machi, Fukushima, Japan

Figure 6a shows the time variation of the trigger rate for 30 min of outdoor measurement. The stability of the trigger rate implies that our Compton camera system operates stably even for measurements conducted outdoors over a long period. To demonstrate how the extended gamma-ray source was reconstructed, we set four different integration periods labelled (i) (1 min), (ii) (10 min), (iii) (20 min) and (iv) (30 min), as shown in **Figure 6a**. **Figure 6b** shows the total energy spectra for each period, depicting the structures superimposed on the photo-absorption peaks of gamma-rays emitted from radioactive nuclides at 605 keV and 796 keV for ^{134}Cs and 662 keV for ^{137}Cs. To reconstruct the gamma-ray image, we selected events within 565-622 keV for 605 keV, 662±40 keV for 662 keV and 796±40 keV for 796 keV. The gamma-ray omnidirectional images for 605, 662 and 796 keV are shown in **Figures 6c-f** for integration periods (i), (ii), (iii) and (iv), respectively. In this case, we find that the reconstructed gamma-ray distribution is stable as long as the integration time exceeds 20 min. The slope of a hill in front and the lower part of rain gutter are clearly contaminated, while the area covered with uncontaminated soil in the right part of image is demonstrably not contaminated. The gamma-ray intensity is in good agreement with dose rate values measured by a scintillation-type survey meter, the values of which are shown in yellow in **Figure 6f**.

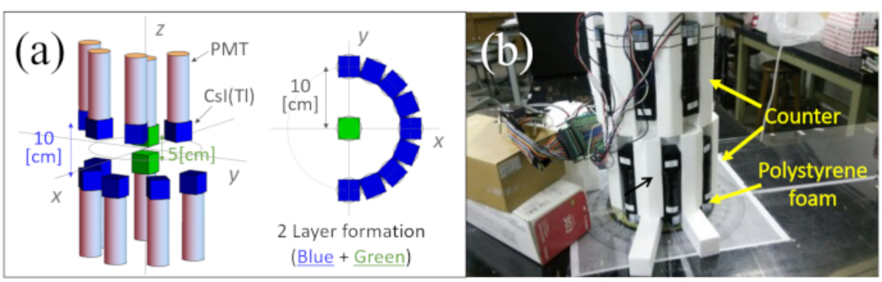

Figure 1: Omnidirectional Gamma-ray imaging Compton camera system. (a) Geometrical arrangement of scintillators with eleven elements used in this study. Two scintillators were arranged at the center of a circle, with nine more arranged in a half-circle, staggered vertically. **(b)** Photograph of the detector without housing. The counters were fixed inside an expanded polystyrene. Please click here to view a larger version of this figure.

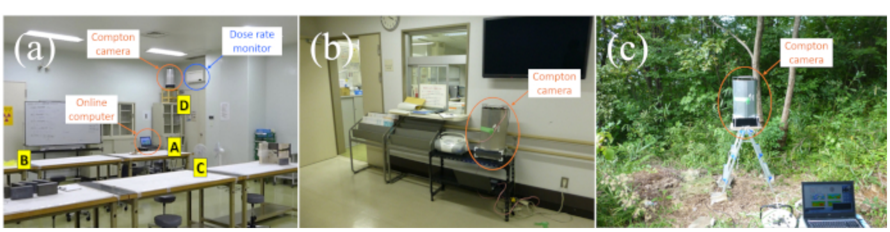

Figure 2: Experimental setup. (a) Monitoring of a sealed radiation source in the experiment room at the RI facility, where a ^{137}Cs-sealed source was sequentially set at the positions labelled 'A', 'B', 'C' and 'D'. **(b)** Environmental monitoring in front of a reception desk in the PET facility. **(c)** Outdoor measurement in the Fukushima field, Japan. The Compton camera was fixed on a stepladder. Please click here to view a larger version of this figure.

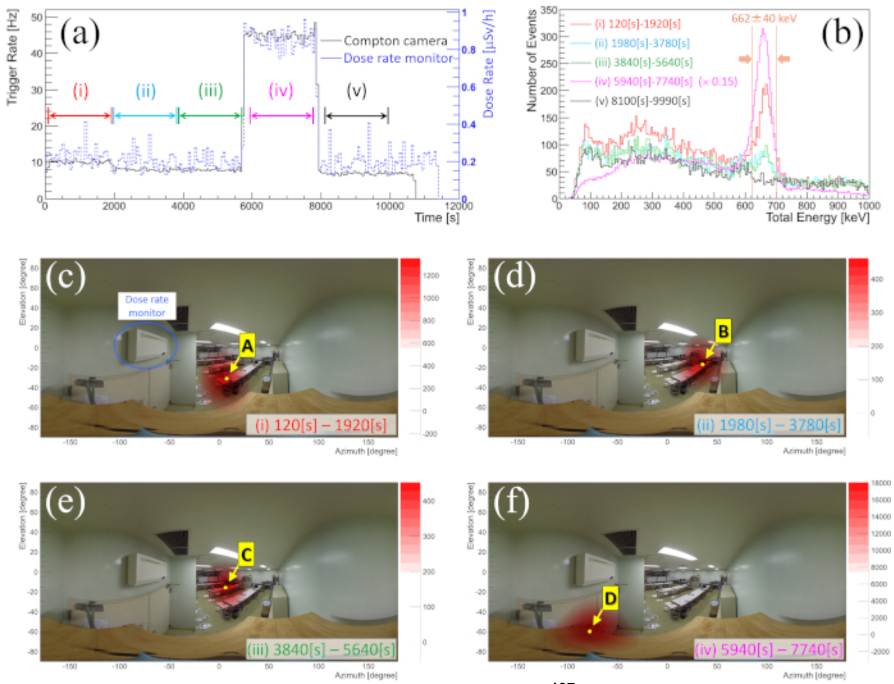

Figure 3: Representative results of the monitoring of a ^{137}Cs-sealed source in the experiment room. (a) Time variation of the trigger rate as measured by the Compton camera (black solid line) and of the air dose rate as measured by the stationary dose rate monitor (blue dashed line). **(b)** Total energy spectra (the sum of energy deposits for each two-fold coincidence event) in **Figure 3a**'s periods (i) (red line), (ii) (blue line), (iii) (green line), (iv) (pink line) and (v) (black line), with the result of (iv) was scaled by 0.15. **(c)** 662 keV gamma-ray omnidirectional image superimposed on the optical image in period (i) (30 min). The red field indicates gamma-ray intensities in the upper half of the observed range. **(d)** Same as **(c)** but for period (ii) (30 min). **(e)** Same as **(c)** but for period (iii) (30 min). **(f)** Same as **(c)** but for period (iv) (30 min). Please click here to view a larger version of this figure.

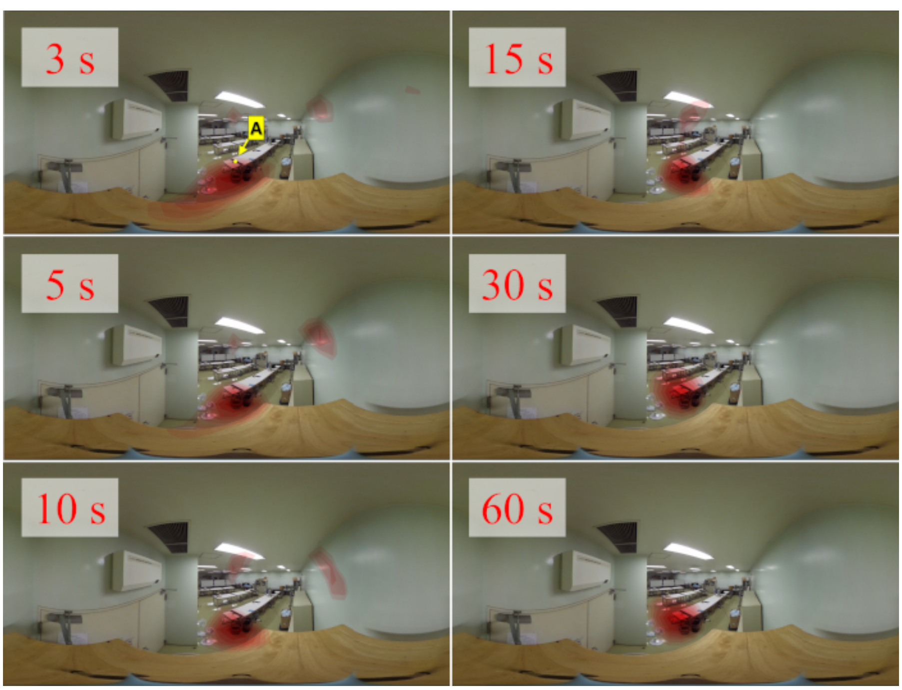

Figure 4: Same as Figure 3c, but with various measurement times: 3 s, 5 s, 10 s, 15 s, 30 s, and 60 s. Here gamma-ray images are identified by the red region, which indicates gamma-ray intensities in the upper 30% of the observed range. Please click here to view a larger version of this figure.

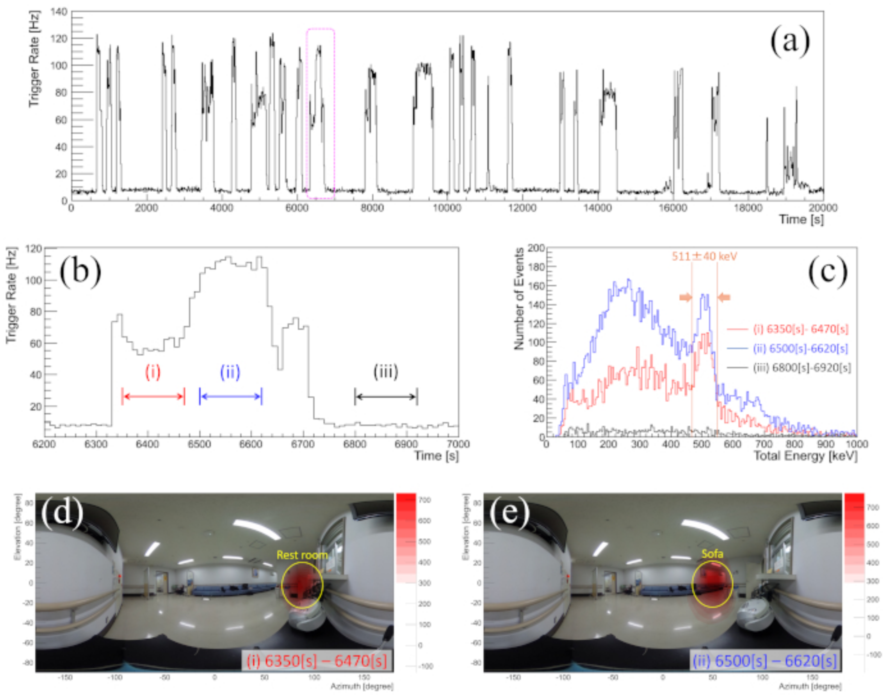

Figure 5: Representative results of environmental monitoring in front of a reception desk in the PET facility. (a) Time variation of the trigger rate as measured by the Compton camera (black line) during the daytime (5.6 h). **(b)** Trigger rate detailed for a period between 6200 s and 7000 s in **(a)**. **(c)** Total energy spectra for **Figure 4b**'s periods (i) (red line), (ii) (blue line) and (iii) (black line). **(d)** 511 keV gamma-ray omnidirectional image superimposed on the optical image for period (i) (2 min). **(e)** Same as **(d)** but for period (ii) (2 min). Please click here to view a larger version of this figure.

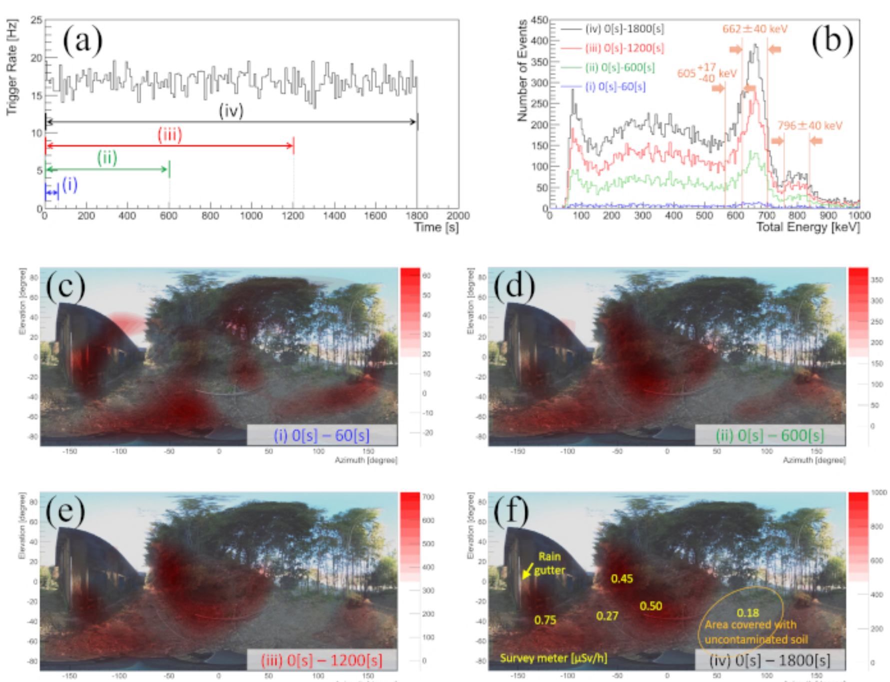

Figure 6: Representative results of outdoor measurement in Kawamata-machi, Fukushima, Japan. (a) Time variation of the trigger rate as measured by the Compton camera (black solid line). **(b)** Total energy spectra for **Figure 5a**'s periods (i) 1 min (blue line), (ii) 10 min (green line), (iii) 20 min (red line) and (iv) 30 min (black line). **(c)** Omnidirectional image of 605, 662 and 796 keV gamma-rays superimposed on the optical image for period (i) (1 min). **(d)** Same as **(c)** but for period (ii) (10 min). **(e)** Same as **(c)** but for period (iii) (20 min). **(f)** Same as **(c)** but for period (iv) (30 min). The dose rate values measured by a scintillation-type survey meter at a height of 1 cm from the ground are shown in the figures for comparison. Please click here to view a larger version of this figure.

	This study	Previous study[18]
Number of counters	11	6
Detection efficiency (cps/(µSv/h)) for 511 keV gamma-rays	36	18
Angular resolution σ (deg)*	11	11

Table 1: Performances of present and previous Compton camera systems. *The angular resolution was estimated from 511 keV omnidirectional gamma ray images obtained during measurement of a ^{22}Na sealed source (0.8MBq) placed 1 m ahead of the detector.

Discussion

We presented three experimental protocols for visualizing various low-level gamma radiation sources using the omnidirectional Compton camera that we developed. The representative results demonstrated that gamma-ray imaging at low radiation levels permits derivation of novel and useful information on the surrounding environment. In the RI facility, the protocol revealed that our Compton camera system successfully discovers the position of the gamma-ray source, as well as the counting rate at the given position relative to the source. This means that the proposed method can serve as a next-generation technology for environmental radiation monitoring, replacing conventional stationary dose rate monitors already mounted on the walls of almost any RI facility. In this paper, we depicted gamma-ray intensity as a red field mapping the region experiencing intensities in the upper half of observed values (**Figure 3**, **Figure 5**, and **Figure 6**), so as to suit various purposes without bias. An approach that rather gives priority to a peak intensity, rather than to the distribution of gamma-ray sources, would adopt a narrower range of the red field, perhaps the upper quarter of observed values, in order to enable directive findings at shorter timescales. Indeed, in **Figure 3c**, the peak direction could be identified with a measurement time of 30 s for case (i) as shown in **Figure 4**, for which the peak position's intensity was around 20 counts.

As for environmental monitoring in the PET facility, the protocol demonstrated the possibility of visualizing the radioactivity movement through the facility, which in this case is considered to be the movement of a patient injected with ^{18}F-FDG. In **Figure 5d,e**, the direction of the patient can be identified in less than 10 s by adopting the narrower red field range as mentioned above. In the future, the environmental monitoring of gamma-ray sources by animation would be useful for various situations, not only for the movement of patients as in this study, but also for monitoring the transfer of nuclear fuel materials such as in airports for purposes of terrorism, by taking advantage of the high-sensitivity and low-cost characteristics of the system, although the energy resolution of a system that uses a scintillator is inferior to that of more expensive semiconductor detectors, such as high purity germanium (HPGe) and CdZnTe (CZT).

In the Fukushima field, the protocol successfully visualized the extended gamma radiation source with surface dose rates of much less than 1 µSv/h, which is an order of magnitude lower than that in a recent report[25,26]. Our Compton camera system was found to be capable of operating stably and robustly for outdoor measurement. We have already confirmed that the system can be operated by using WiFi and portable battery for more convenient use in various situations, especially for outdoor measurement. The Ministry of Environment in Japan has set the air dose rate minimum at 0.23 µSv/h to designate areas to be decontaminated. We believe that our system and protocols will be a great help for the decontamination procedure in areas of low-level radioactive contamination in broad areas of eastern Japan where radioactive cesium was released by the Fukushima Daiichi nuclear power plant accident in 2011.

The Compton camera used in this study has high sensitivity for gamma rays with energies between 300 keV and 1400 keV, attributable to the use of 3.5 cm CsI(Tl) scintillator cubes[18]. Scintillator type and size can be optimized for environmental monitoring of low-level gamma radiation sources below 300 keV, such as ^{99m}Tc (141 keV) and ^{111}In (171 keV, 245 keV), which are frequently used in scintigraphy. This work will be presented in another paper in the near future. The detector can be manufactured at a low price. In fact, the cost of the detector materials used in this study was no more than $20,000, and this amount was dominated by the price of the counter consisting of CsI (Tl) and PMT; this configuration is significantly less expensive than the GAGG scintillators and HPGe semiconductor detectors that are used in other Compton cameras. Furthermore, the system used in this study should be made more compact for the sake of versatility and convenience. The size of the system produced in this study was 30 cm x 25 cm x 40 cm, which is larger than the existing portable gamma camera[5,27]. The main reasons for such large system size are the large size of the PMT attached to CsI (Tl) (φ4 cm × 12 cm) and the large electronics handmade by us. In the future, portability will be improved by replacing the PMT with a metal package PMT or Silicon Photomultiplier (SiPM) as well as by repackaging the electronics at small size.

Disclosures

The authors have nothing to disclose.

Acknowledgments

This study was supported by the Open Source Consortium of Instrumentation (Open-It), Japan, JSPS KAKENHI Grant (Nos. 22244019, 26610055, 15H04769 and 19H04492).

References

1. ICRP. 1990 Recommendations of the international commission on radiological protection. *Annals of the ICRP.* **21**, ICRP Publication 60 (1991).

2. Kamae, T., Enomoto, R., Hanada, N. A new method to measure energy, direction, and polarization of gamma rays. *Nuclear Instruments and Methods in Physics Research Section A: Accelerators, Spectrometers, Detectors and Associated Equipment.* **260**, 254-257 (1987).
3. Schoenfelder, V. et al. Instrument description and performance of the imaging gamma-ray telescope COMPTEL aboard the Compton Gamma-ray Observatory. *The Astrophysical Journal Supplement Series.* **86**, 657-692 (1993).
4. Suzuki, Y. et al. Three-dimensional and multienergy gamma-ray simultaneous imaging by Using a Si/CdTe compton camera. *Radiology.* **267**, 941-947 (2013).
5. Kataoka, J. et al. Recent progress of MPPC-based scintillation detectors in high precision X-ray and Gamma-ray imaging. *Nuclear Instruments and Methods in Physics Research Section A: Accelerators, Spectrometers, Detectors and Associated Equipment.* **784**, 248-254 (2015).
6. Tanimori, T., et al. Establishment of imaging spectroscopy of nuclear gamma-rays based on geometrical optics. *Scientific Reports.* **7**, 41511 (12pp) (2017).
7. Sakai, M., et al. In vivo simultaneous imaging with ^{99m}Tc and ^{18}F using a Compton camera. *Physics in Medicine & Biology.* **63**, 205006 (12pp) (2018).
8. Koide, A., et al. Precision imaging of 4.4 MeV gamma rays using a 3-D position sensitive Compton camera. *Scientific Reports.* **8**, 8116 (9pp) (2018).
9. Nagao, Y., et al. Astatine-211 imaging by a Compton camera for targeted radiotherapy. *Applied Radiation and Isotopes.* **139**, 238-243 (2018).
10. Draeger, E., et al. 3D prompt gamma imaging for proton beam range verification, *Physics in Medicine & Biology.* **63**, 35019 (13pp) (2018).
11. Uenomachi, M., et al. Double photon emission coincidence imaging with GAGG-SiPM Compton camera. *Nuclear Instruments and Methods in Physics Research Section A: Accelerators, Spectrometers, Detectors and Associated Equipment.* in press (2019).
12. Nakano, T., et al. Imaging of ^{99m}Tc-DMSA and ^{18}F-FDG in Humans Using a Si/CdTe Compton Camera. *Physics in Medicine & Biology.* in press (2019).
13. Lee, W., Lee, T. 4 p FOV compact Compton camera for nuclear material investigations. *Nuclear Instruments and Methods in Physics Research Section A: Accelerators, Spectrometers, Detectors and Associated Equipment.* **652**, 33-36 (2011).
14. Yamaya, T., et al. Concrete realization of the whole gamma imaging concept, *Proceedings of 2017 IEEE Nuclear Science Symposium and Medical Imaging Conference (NSS/MIC).* 3pp (2017).
15. Parra, L. Reconstruction of cone-beam projections from Compton scattered data, *IEEE Transactions on Nuclear Science.* **47**, 1543-1550 (2000).
16. Xu, D., He, Z. Filtered Back-Projection in 4p Compton Imaging with a Single 3D Position Sensitive CdZnTe Detector. *IEEE Transactions on Nuclear Science.* **53**, 2787-2795 (2006).
17. Wilderman, S., Clinthorne, N., Fessler, J., Rogers, W. List-mode maximum likelihood reconstruction of Compton scatter camera images in nuclear medicine, *Proceedings of IEEE Nuclear Science Symposium.* **3**, 1716-1720 (1998).
18. Watanabe, T., et al. Development of an omnidirectional gamma-ray imaging Compton camera for low-radiation-level environmental monitoring. *Japanese Journal of Applied Physics.* **57**, 026401 (2018).
19. Kagaya, M., et al. Development of a low-cost-high-sensitivity Compton camera using CsI(Tl) scintillators (γI). *Nuclear Instruments and Methods in Physics Research Section A: Accelerators, Spectrometers, Detectors and Associated Equipment.* **804**, 25-32 (2015).
20. Muraishi, H., Kagaya, M., Katagiri, H., Takeda, T., Watanabe, T. Proposal of a new image reconstruction technique for the Compton camera. *The Journal of Japan Academy of Health Science.* **17**, 159-164 (2014).
21. Katagiri, H., et al. Development of an all-sky gamma-ray Compton camera based on scintillators for high-dose environments. *Journal of Nuclear Science and Technology.* **55**, 1172-1179 (2018).
22. Watanabe, T., et al. Remote measurement of urinary radioactivity in ^{18}F-FDG PET patients using Compton camera for accuracy evaluation of standardized uptake value. *Biomedical Physics & Engineering Express.* **4**, 065029 (5pp) (2018).
23. Uchida, T. Hardware-based TCP processor for gigabit ethernet. *IEEE Transactions on Nuclear Science.* **55**, 1631-1637 (2008).
24. Brun, R., Redemakers, R. ROOT - An Object-Oriented Data Analysis Framework. *Nuclear Instruments and Methods in Physics Research Section A: Accelerators, Spectrometers, Detectors and Associated Equipment.* **389**, 81-86 (1997).
25. Tomono, D., et al. First on-site true gamma-ray imaging-spectroscopy of contamination near Fukushima plant. *Scientific Reports.* **7**, 41972 (10pp) (2017).
26. Kataoka, J., et al. Ultracompact Compton camera for innovative gamma-ray imaging. *Nuclear Instruments and Methods in Physics Research Section A: Accelerators, Spectrometers, Detectors and Associated Equipment.* **912**, 1-5 (2018).
27. Wahl, C. G., et al. The Polaris-H imaging spectrometer. *Nuclear Instruments and Methods in Physics Research Section A: Accelerators, Spectrometers, Detectors and Associated Equipment.* **784**, 377-381 (2015).